DNA binding, DNA cleavage, antioxidant and cytotoxicity studies on ruthenium(II) complexes of benzaldehyde 4-methyl-3-thiosemicarbazones

Krishnan Sampath, Subbaiyan Sathiyaraj, Chinnasamy Jayabalakrishnan

PII: S1386-1425(12)01299-1
DOI: http://dx.doi.org/10.1016/j.saa.2012.12.064
Reference: SAA 10116

To appear in: *Spectrochimica Acta Part A: Molecular and Biomolecular Spectroscopy*

Received Date: 26 October 2012
Revised Date: 7 December 2012
Accepted Date: 10 December 2012

Please cite this article as: K. Sampath, S. Sathiyaraj, C. Jayabalakrishnan, DNA binding, DNA cleavage, antioxidant and cytotoxicity studies on ruthenium(II) complexes of benzaldehyde 4-methyl-3-thiosemicarbazones, *Spectrochimica Acta Part A: Molecular and Biomolecular Spectroscopy* (2012), doi: http://dx.doi.org/10.1016/j.saa.2012.12.064

DNA binding, DNA cleavage, antioxidant and cytotoxicity studies on ruthenium(II) complexes of benzaldehyde 4-methyl-3-thiosemicarbazones

Krishnan Sampath, Subbaiyan Sathiyaraj and Chinnasamy Jayabalakrishnan*

Post-Graduate and Research Department of Chemistry, Sri Ramakrishna Mission Vidyalaya College of Arts and Science, Coimbatore – 641 020, Tamil Nadu, India.

ABSTRACT

Four new ruthenium(II) complexes with N(4)-methyl thiosemicarbazone ligands, (E)-2-(2-chlorobenzylidene)-N-methylhydrazinecarbothioamide (HL^1) and (E)-N-methyl-2-(2-nitrobenzylidene)hydrazinecarbothioamide (HL^2), were prepared and fully characterized by various spectro-analytical techniques. The Schiff bases act as bidentate, monobasic chelating ligands with S and N as the donor sites and are preferably found in the thiol form in all the complexes studied. The molecular structure of HL^1 and HL^2 were determined by single crystal X-ray diffraction method. DNA binding of the compounds was investigated by absorption spectroscopy which indicated that the complexes bind to DNA *via* intercalation. The oxidative cleavage of the complexes with CT-DNA inferred that the effects of cleavage are dose dependent. Antioxidant studies of the ligands and complexes showed the significant antioxidant activity against DPPH radical. In addition, the *in vitro* cytotoxicity of the ligands and complexes against MCF-7 cell line was assayed which showed higher cytotoxic activity with the lower IC_{50} values indicating their efficiency in killing the cancer cells even at low concentrations.

Keywords: Ruthenium(II) complexes, Thiosemicarbazones, DNA interaction, Antioxidant, Cytotoxicity.

1. Introduction

Cancer is one of the fatal diseases, which claims over 6 million people each year worldwide and still increasing. The majority of drugs used for the treatment of cancer today are not 'cancer cell-specific' and potently cytotoxic against normal cells. So, the most rapidly developing area of pharmaceutical research is the discovery of new drugs for cancer today. To date, cisplatin is considered to be one of the most effective and widely used anticancer drugs. Second generation platinum drugs including cisplatin and oxaliplatin have been developed for clinical application [1]. The efficacy of these drugs, including cisplatin,

however, is reduced by increasing tumour resistance and in the case of cisplatin, high toxicity. This in turn affects the administration of the drugs [2]. These limitations have aroused interest towards the design and evaluation of transition metal complexes other than platinum derivatives for therapeutic use. In this respect ruthenium complexes, due to their favourable properties viz. kinetic ligand-exchange, variable oxidation states and lower toxicity toward normal cells (due to similarity with iron), are in the forefront of these investigations [3,4].

Thiosemicarbazones are versatile ligands as they possess a number of donor atoms which may coordinate in various ways. In addition to this, thiosemicarbazones possess a variety of biological properties including antiproliferative activity [5,6]. Studies have demonstrated that thiosemicarbazones are potent inhibitors of the enzyme ribonucleotide reductase and are capable of interrupting DNA synthesis and repair. Incorporation of metals onto these thiosemicarbazone ligands can result in alteration or enhancement of their biological activity [7,8]. In the case of pharmaceuticals, the binding capacity of thiosemicarbazones is further increased by condensation of the thiosemicarbazide with an aldehyde containing heteroatom [9,10]. This aroused our interest in the synthesis of benzaldehyde thiosemicarbazones and their ruthenium(II) complexes with a viewpoint towards evaluating biological properties such as DNA interaction, antioxidant and cytotoxic activity. Herein, we report the synthesis, characterization, DNA binding, DNA cleavage, antioxidative and cytotoxicity studies of ruthenium(II) complexes of 2-choloro/nitro benzaldehyde 4-methyl-3-thiosemicarbazones. The crystal structure of the thiosemicarbazone ligands have been determined by X-ray crystallography. The investigation of the biological properties of the ligands and ruthenium(II) complexes has been focused on the binding properties with CT-DNA performed by UV spectroscopy and cleavage properties of the complexes performed by gel electrophoresis with CT-DNA. Finally, we have studied their antioxidative property against DPPH radical and *in vitro* antitumor activity against MCF-7 cancer cell line.

2. Experimental

2.1. Materials and Methods

All the chemicals used were chemically pure and AR grade. Solvents were purified and dried according to the standard procedure [11]. Calf-thymus (CT-DNA) was purchased from Bangalore Genei, Bangalore, India. The metal precursors [$RuHCl(CO)(PPh_3)_3$]

and [RuHCl(CO)($AsPh_3$)$_3$] were prepared by literature methods [12,13]. Micro analyses (C, H, N & S) were performed on a Vario EL III CHNS analyser at STIC, Cochin University of Science and Technology, Kerala, India. IR spectra were recorded as KBr pellets in the 400-4000 cm^{-1} region using a Perkin Elmer FT-IR 8000 spectrophotometer. Electronic spectra were recorded in DMSO solution with a Systronics double beam UV-vis spectrophotometer 2202 in the range 200-800 nm. ^{1}H NMR and ^{13}C NMR spectra were recorded on a Bruker AV III 500 MHZ instrument using TMS as an internal reference. ^{31}P NMR spectra were recorded on a Bruker AV III 500 MHZ instrument using ortho phosphoric acid as an internal reference. Antioxidant and anti cancer studies were carried out at the Kovai Medical Centre and Hospital Pharmacy College, Coimbatore, Tamilnadu. Melting points were recorded with Veego VMP-DS heating table.

2.2. Preparation of thiosemicarbazone ligands

*2.2.1. (E)-2-(2-chlorobenzylidene)-N-methylhydrazinecarbothioamide (HL^1) (**1**)*

A methanolic solution (50 mL) of 4-methyl-3-thiosemicarbazide (1.051 g, 0.01 mol) was added to a methanol solution (25 mL) containing 2-chlorobenzaldehyde (1.12 mL, 0.01 mol). The mixture was refluxed for an hour during which period a white color precipitate was formed. The reaction was cooled to room temperature and the solid compound was filtered, washed and recrystallized from methanol. White colored crystals, suitable for single crystal X-ray diffraction analysis, were obtained by slow evaporation of its methanolic solution. Yield: 89%; M.P: 200-201 °C. Anal. calcd. for $C_9H_{10}ClN_3S$ (%): C, 47.47; H, 4.43; N, 18.45; S, 14.08. Found (%): C, 47.40; H, 4.45; N, 18.43; S, 14.01. IR (KBr, cm^{-1}): 1585 ν(C=N); 951 ν(C=S). UV-vis (DMSO), λmax (nm) (ε M^{-1} cm^{-1}): 305 (11400), 360 (14233) ($\pi \rightarrow \pi^*$, $n \rightarrow \pi^*$). ^{1}H NMR (DMSO-d_6); δ 8.60 (s, 1H, hydrazine NH); δ 8.47 (s, 1H, methyl NH); δ 11.67 (s, 1H, H–C=N); δ 3.03 (d, 3H, CH_3); δ 7.39-8.30 (m, 4H, aromatic). ^{13}C NMR (DMSO-d_6); δ 142 (C=S); δ 178 (C=N); δ 31 (CH_3); δ 127-133 (aromatic).

*2.2.2. (E)-N-methyl-2-(2-nitrobenzylidene)hydrazinecarbothioamide (HL^2) (**2**)*

It was prepared by using the same procedure as described for HL^1 with 4-methyl-3-thiosemicarbazide (1.051 g, 0.01 mol) and 2-nitrobenzaldehyde (1.511 g, 0.01 mol). A yellow product was formed. The solid compound was filtered, washed and recrystallized from methanol. Yellow colored crystals, suitable for single crystal X-ray diffraction analysis, were obtained by slow evaporation of its methanolic solution.

Yield: 85%; M.P: 229-230 °C. Anal. calcd. for $C_9H_{10}N_4O_2S$ (%): C, 45.37; H, 4.23; N, 23.51; S, 13.46. Found (%): C, 45.39; H, 4.29; N, 23.52; S, 13.42. IR (KBr, cm^{-1}): 1530 ν(C=N); 850 ν(C=S). UV-vis (DMSO), λmax (nm) (ε M^{-1} cm^{-1}): 305 (11466), 368 (14744), 396 (20955) ($\pi \rightarrow \pi^*$, $n \rightarrow \pi^*$). ^{1}H NMR (DMSO-d_6); δ 8.64 (s, 1H, hydrazine NH); δ 8.48 (s, 1H, methyl NH); δ 11.79 (s, 1H, H–C=N); δ 3.04 (d, 3H, CH_3); δ 7.61-8.43 (m, 4H, aromatic). ^{13}C NMR (DMSO-d_6); δ 148 (C=S); δ 178 (C=N); δ 31 (CH_3); δ 125-137 (aromatic).

2.2.3. Single crystal X-ray diffraction studies.

Single crystal X-ray diffraction data of **1** and **2** were collected at room temperature on a Bruker AXS KAPPA APEX2 CCD diffractometer equipped with a fine focused sealed tube. The unit cell parameters were determined and the data collections of ligands **1** and **2** were performed using a graphite-mono chromate Mo Kα (λ = 0.71073 Å) radiation by φ and ω scans. The data collected were reduced SAINT program [14] and the empirical absorption corrections were carried out using the SADABS program [15]. The structure of the compounds **1** and **2** was solved by direct methods [16] using SHELXS-97, which revealed the position of all non-hydrogen atoms, and was refined by full-matrix least squares on F^2 (SHELXL-97) [17]. All non-hydrogen atoms were refined anisotropically, while the hydrogen atoms were placed in calculated positions and refined as riding atoms.

2.3. Preparation of ruthenium(II) complexes

*2.3.1. Synthesis of [RuCl(CO)(PPh_3)$_2$$L^1$] (**3**)*

A methanolic solution (20 mL) containing HL^1 (**1**) (0.110 g, 0.5 mmol) and triethylamine (0.07 mL, 0.5 mmol) were added to [RuHCl(CO)(PPh_3)$_3$] (0.475 g, 0.5 mmol) in benzene (20 mL). The resulting red color solution was refluxed for 8 h. The reaction mixture was then cooled to room temperature, which results in the formation of orange color precipitate. It was filtered off and then subjected to purification by TLC. This solid was recrystallized from CH_2Cl_2/Hexane mixture. Our sincere effort to obtain single crystal of the complexes went unsuccessful. Yield: 59%. M.P: 230-232 °C. Anal. calcd. for $C_{46}H_{39}Cl_2N_3OP_2RuS$ (%): C, 60.33; H, 4.29; N, 4.59; S, 3.50. Found (%): C, 60.31; H, 4.21; N, 4.55; S, 3.58. IR (KBr, cm^{-1}): 1575 ν(C=N); 745 ν(C–S); 1948 ν(C≡O). UV-vis (DMSO), λmax (nm) (ε M^{-1} cm^{-1}): 305 (11455), 368 (14866) (ILCT), 404 (19866) (MLCT). ^{1}H NMR (DMSO-d_6); δ 8.47 (s, 1H, methyl NH); δ 11.69 (s, 1H, H–C=N); δ 3.03 (d, 3H, CH_3);

δ 7.24-8.31 (m, 34H, aromatic). ^{13}C NMR (DMSO-d_6); δ 137 (C–S); δ 181 (C=N); δ 194 (C≡O); δ 31 (CH_3); δ 125-134 (aromatic). ^{31}P NMR (DMSO-d_6); δ 36.3 (PPh_3).

*2.3.2. Synthesis of [RuCl(CO)($AsPh_3$)$_2$L^1] (**4**)*

It was prepared by using the same procedure as described for **3** with HL^1 (**1**) (0.110 g, 0.5 mmol) and [RuHCl(CO)($AsPh_3$)$_3$] (0.540 g, 0.5 mmol). Yellow colored powder obtained. Yield: 55%. M.P: 238-240 °C. Anal. calcd. for $C_{46}H_{39}Cl_2N_3OAs_2RuS$ (%): C, 55.05; H, 3.92; N, 4.19; S, 3.19. Found (%): C, 55.15; H, 3.95; N, 4.15; S, 3.12. IR (KBr, cm^{-1}): 1567 ν(C=N); 735 ν(C–S); 1939 ν(C≡O). UV-vis (DMSO), λmax (nm) (ε M^{-1} cm^{-1}): 305 (11533), 368 (14877) (ILCT), 404 (19622) (MLCT). ^{1}H NMR (DMSO-d_6); δ 8.46 (s, 1H, methyl NH); δ 11.68 (s, 1H, H–C=N); δ 3.03 (d, 3H, CH_3); δ 7.24-8.30 (m, 34H, aromatic). ^{13}C NMR (DMSO-d_6); δ 138 (C–S); δ 182 (C=N); δ 191 (C≡O); δ 31 (CH_3); δ 127-133 (aromatic).

*2.3.3. Synthesis of [RuCl(CO)(PPh_3)$_2$L^2] (**5**)*

It was prepared by using the same procedure as described for **3** with HL^2 (**2**) (0.138 g, 0.5 mmol) and [RuHCl(CO)(PPh_3)$_3$] (0.475 g, 0.5 mmol). Brown colored powder obtained. Yield: 58%. M.P: 248-250 °C. Anal. calcd. for $C_{46}H_{39}ClN_4O_3P_2RuS$ (%): C, 59.64; H, 4.24; N, 6.05; S, 3.46. Found (%): C, 59.69; H, 4.27; N, 6.00; S, 3.42. IR (KBr, cm^{-1}): 1519 ν(C=N); 744 ν(C–S); 1947 ν(C≡O). UV-vis (DMSO), λmax (nm) (ε M^{-1} cm^{-1}): 305 (11500), 368 (14566), 401 (18388) (ILCT), 431 (20855) (MLCT). ^{1}H NMR (DMSO-d_6); δ 8.48 (s, 1H, methyl NH); δ 11.81 (s, 1H, H–C=N); δ 3.03 (d, 3H, CH_3); δ 7.23-8.18 (m, 34H, aromatic). ^{13}C NMR (DMSO-d_6); δ 138 (C–S); δ 182 (C=N); δ 192 (C≡O); δ 31 (CH_3); δ 125-133 (aromatic). ^{31}P NMR (DMSO-d_6); δ 36.3 (PPh_3).

*2.3.4. Synthesis of [RuCl(CO)($AsPh_3$)$_2$L^2](**6**)*

It was prepared by using the same procedure as described for **3** with HL^2 (**2**) (0.138 g, 0.5 mmol) and [RuHCl(CO)($AsPh_3$)$_3$] (0.54 g, 0.5 mmol). Orange colored powder obtained. Yield: 56%. M.P: 263-265 °C. Anal. calcd. for $C_{46}H_{39}ClN_4O_3As_2RuS$ (%): C, 54.57; H, 3.88; N, 5.52; S, 3.16. Found (%): C, 54.52; H, 3.80; N, 6.55; S, 3.19. IR (KBr, cm^{-1}): 1520 ν(C=N); 737 ν(C–S); 1949 ν(C≡O). UV-vis (DMSO), λmax (nm) (ε M^{-1} cm^{-1}): 305 (11577), 368 (14933), 404 (19977) (ILCT), 432 (20855) (MLCT). ^{1}H NMR (DMSO-d_6); δ 8.49 (s, 1H, methyl NH); δ 11.81 (s, 1H, H–C=N); δ 3.03 (d, 3H, CH_3); δ 7.27-8.19

(m, 34H, aromatic). ^{13}C NMR (DMSO-d_6); δ 139 (C–S); δ 181 (C=N); δ 192 (C≡O); δ 31 (CH_3); δ 128-133 (aromatic).

2.4. DNA binding - Titration experiments

All the experiments involving the binding of compounds with CT-DNA were carried out in a doubly distilled water buffer with tris(hydroxymethyl)-aminomethane (Tris, 5 mM) and sodium chloride (50 mM) and adjusted to pH 7.2 with hydrochloric acid. A solution of CT-DNA in the buffer gave a ratio of UV absorbance of about 1.8-1.9 at 260 and 280 nm, indicating that the DNA was sufficiently free of protein. The CT-DNA concentration per nucleotide was determined spectrophotometrically by employing an extinction coefficient of 6600 M^{-1} cm^{-1} at 260 nm. The compounds were dissolved in a mixed solvent of 5 % DMSO and 95 % Tris-HCl buffer. Stock solutions were stored at 4 °C and used within 4 days. Absorption titration experiments were performed with fixed concentrations of the complexes (25 µM) with varying concentration of DNA (0-40 µM). While measuring the absorption spectra, an equal amount of DNA was added to both the test solution and the reference solution to eliminate the absorbance of DNA itself.

2.5. Nuclease activity using gel electrophoresis

The DNA cleavage activity of the ruthenium(II) complexes was monitored by agarose gel electrophoresis on CT DNA. The tests were performed in the absence and presence of activating agent, H_2O_2 under aerobic condition. Hydrolytic cleavage was monitored by 30 µM of CT DNA and 40 µM of each complex (**3**-**6**) in 5 % DMSO and 95 % Tris-HCl buffer (5 mM, pH 7.2) with 50 mM NaCl.

For oxidative cleavage, each reaction mixture contained 30 µM of CT DNA, 30; 60; 90 µM of each complex (**3**-**6**) in 5 % DMSO and 95 % Tris-HCl buffer (5 mM, pH 7.2) with 50 mM NaCl and 60 µM of H_2O_2.

The samples with sufficient buffer were incubated for 2 h at 37 ^oC. After incubation, 1 µL of loading buffer (0.25 % bromophenol blue, 0.25 % xylene cynol and 60 % glycerol) was added to the reaction mixture and loaded onto a 1 % agarose gel containing 1.0 µg/mL of ethidium bromide. The electrophoresis was carried out for 2 h at 50 V in Tris-acetic acid EDTA buffer. The bands were visualized under UV light and photographed.

2.6. Antioxidant activity

The 2,2-diphenyl-2-picryl-hydrazyl (DPPH) radical scavenging activity of the compounds was measured according to the method of Elizabeth [18]. The DPPH radical is a stable free radical having a λ_{max} at 517 nm. A fixed concentration of the experimental compound (100 µL) was added to a solution of DPPH in methanol (0.3 mM, 1 mL) and the final volume was made up to 4 mL with double distilled water. DPPH solution with methanol was used as a positive control and methanol alone acted as a blank. The solution was incubated at 37 °C for 30 min in dark. The decrease in absorbance of DPPH was measured at 517 nm. The tests were run in triplicate, and various concentrations (20-100 µg/ mL) of the compounds used to fix a concentration at which the compounds showed 50 % of activity. In addition, the percentage of activity was calculated using the formula, % of suppression ratio = $[(A_0 – A_c)/A_0]$ X 100. A_0 and A_c are the absorbance in the absence and presence of the tested compounds respectively. The 50 % activity (IC_{50}) can be calculated using the percentage of activity.

2.7. In vitro anticancer activity assay

Cytotoxicity of the compounds were carried out on human breast cancer cell line (MCF-7) was obtained from National Centre for Cell Science (NCCS), Pune, India. Cell viability was carried out using the MTT assay method [19]. MCF-7 cell was grown in eagles minimum essential medium (EMEM) containing 10 % fetal bovine serum (FBS). For the screening experiment, the cells were seeded onto 96-well plates at plating density of 10,000 cells/ well and incubated to allow for cell attachment at 37 °C, 5 % CO_2, 95 % air and 100 % relative humidity for 24 h prior to the addition of the compounds. The compounds were dissolved in DMSO and diluted in the respective medium containing 1 % FBS. After 24 h the medium was replaced with the respective medium with 1 % FBS containing the compounds at various concentrations and incubated at 37 °C under conditions of 5 % CO_2, 95 % air and 100 % relative humidity for 48 h. Triplication was maintained and the medium not containing the compounds served as control. After 48 h, 15 µL of MTT (5 mg mL^{-1}) in phosphate buffered saline (PBS) was added to each well and incubated at 37 °C for 4 h. The medium with MTT was then removed and the formed formazan crystals were dissolved in 100 µL of DMSO. The absorbance was then measured at 570 nm using micro plate reader. The % cell inhibition was determined using the following formula and a graph was plotted with the percentage of cell inhibition *versus* concentration. From this, the IC_{50} was

calculated: % cell Inhibition = [mean OD of untreated cells (control)/mean OD of treated cells (control)] x100.

3. Results and Discussion

Analytical and spectroscopic data for the ligands and its complexes indicate a 1:1 metal-ligand stoichiometry for all the complexes. The synthetic route of the complexes and the proposed structure of the complexes are shown in Scheme 1. The complexes are soluble in most common organic solvents like CH_2Cl_2, $CHCl_3$, DMF, DMSO, etc.

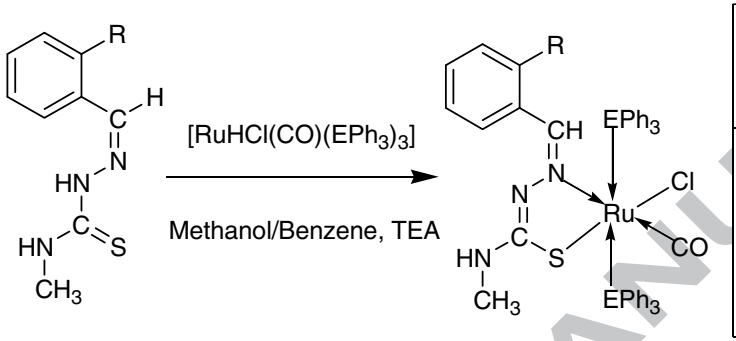

Ligand	R
HL^1	Cl
HL^2	NO_2

Scheme 1 Synthetic route of the ruthenium(II) thiosemicarbazone complexes, where E=P/As.

3.1. X-ray crystallography

The ORTEP representation of compounds **1** and **2** is shown in Fig. 1 and 2 respectively. Relevant data collection and details of the structure refinement are summarized in Table 1. The selected bond lengths, bond angles and torsion angles for compounds **1** and **2** are given in tables 2, 3 and 4 respectively.

The ligand **1** crystallizes in a monoclinic space group C_2/c with eight crystallographically independent molecules in the unit cell (Fig 3). Its existence in the thione form is confirmed by the C=S bond length of 1.6884(14) Å. The molecule exists in the E conformation about N2-N3 bond as evidenced by the C2-N2-N3-C3 torsion angle of 175.6(1)°. The azomethine bond length, C3-N3 (1.276(2) Å) is in conformity with a formed C=N double bond length (1.28 Å). The ligand **2** crystallizes in a triclinic space group P-1 with two crystallographically independent molecules in the unit cell (Fig. 4). The azomethine bond length, C7-N2 (1.276(1) Å) is in conformity with a formal C=N double bond length (1.28 Å) and C8-S1 bond distance of 1.683(1) Å is very close to a formal C=S bond length (1.60 Å). It confirms the existence of the thiosemicarbazone in the thione form in the solid

state. The thione sulphur atom S(1) is trans to the azomethine nitrogen atom N(2) which confirmed by a torsion angle of 179.68(8) for S(1)-C(8)-N(3)-N(2) bond.

3.2. Infrared spectra

The IR spectra of the free ligands were compared with those of the metal complexes in order to study the binding mode(s) of the thiosemicarbazone ligand to metal. A medium sharp band at 1530 and 1585 cm^{-1} due to the azomethine C=N stretching frequency of the free ligands **1** and **2** respectively was shifted to lower frequency in the spectra of the complexes at 1519-1575 cm^{-1} indicating that the coordination through N atom [20]. A band appeared at 951 cm^{-1} for **1** and 850 cm^{-1} for **2** due to vibration of the C=S double bond which disappeared in the spectra of the complexes and a new band, C–S appeared at 735-745 cm^{-1} indicating that the other coordination is through thiolate sulphur after enolization followed by deprotonation on sulphur [21]. Further, the replacement of hydride ion in the metal precursors by the ligands has been confirmed by the absence of a band around 2020 cm^{-1} in all the complexes [22]. In all the complexes, the strong band in the region 1939-1949 cm^{-1} is due to terminally coordinated carbonyl group. Overall, the complexes contain monobasic NS coordinated thiosemicarbazones. In addition, the characteristic absorption bands due to triphenylphosphine and triphenylarsine were also observed for all the complexes in their expected regions.

3.3. Electronic spectra

The electronic spectra of the ligands show bands at 305, 360-396 nm. The first band at 305 nm, is assigned to a ligand $\pi \rightarrow \pi^*$ transition, while the band at 360-396 nm is assigned to an $n \rightarrow \pi^*$ transition associated with the imine and thioamide function of the thiosemicarbazones. The spectra of the complexes showed three to four bands in the region 303-432 nm. The bands at 303-308 and 368 nm were associated with intra ligand transitions. These bands are shifted when compared to ligands indicating the involvement of imine nitrogen and thionyl sulphur in coordination with ruthenium atom [21]. The bands appearing in the region 401-432 nm have been assigned to charge transfer transitions arising from the excitation of an electron from metal t_{2g} level to an unfilled molecular orbital derived from the π^* level of the ligands [22]. The pattern of the electronic spectra for the complexes are similar to other ruthenium(II) octahedral complexes [23,24].

3.4. NMR spectra

The NMR spectra of the compounds were recorded in DMSO-d_6 solution for confirming the binding mode of the ligands to the ruthenium ion and the ^{1}H, ^{13}C and ^{31}P NMR spectra of the complex **3** are shown in Fig. 5. The ^{1}H NMR spectra of the free ligands showed a singlet in the region δ 8.60-8.64 for the hydrazine NH proton, which is absent in the spectra of the complexes indicating the enolization and deprotonation of the –NH–C=S group prior to coordination of ligand to metal through thiolate sulphur. The –CH=N proton observed at δ 11.67-11.79 in the spectra of the ligands, is shifted slightly downfield in the spectra of the complexes in the region δ 11.68-11.81. This observation supports the involvement of –C=N chromophore in coordination. The aromatic protons, observed as multiplets in the region δ 7.39-8.43 in the spectra of the ligands, are remain more or less unchanged in the complexes in the region δ 7.23-8.43, due to the delocalisation of electron density in the system [25] and these signals in the complexes cannot be distinguished from the aromatic signals of PPh_3/ $AsPh_3$ due to their extensive overlap [23]. For ligands and complexes, the chemical shift at δ 3.03-3.04 and δ 8.46-8.49 are due to methyl proton and methyl NH proton respectively.

In the ^{13}C NMR spectra of the ligands, the signal at δ 142-148 corresponds to the thioamide carbon (C=S), which disappears in the spectra of the complexes and a new signal, (C–S) at δ 137-139 indicates the coordination of sulphur *via* deprotonation [24]. The spectra of the ligands displayed a single resonance at δ 178 due to the azomethine carbon atom, downfield shift of this signal at δ 181-182 clearly indicates the coordination of C=N carbon atom. The aromatic carbons of the free ligands and complexes show signal in the region δ 125-137. The signal due to methyl carbon of ligands and the complexes appear at δ 31. For all the complexes, the terminal carbonyl group C≡O appeared at δ 191-194 [26].

In order to confirm the presence of triphenylphosphine group, ^{31}P NMR spectra were recorded for the complexes, **3** and **5**. A sharp singlet was observed at δ 36.3 ppm for the complexes, **3** and **5** due to presence of magnetically equivalent phosphorous atoms suggesting the presence of two triphenylphosphine groups in a position trans to each other [27].

3.5. Pharmacology

3.5.1. DNA binding - Titration experiments

The study of non-covalent interactions of transition metal complexes with DNA is an area of intense current interest. Because DNA is an important cellular receptor, many compounds exert their anticancer effects through binding to DNA, thereby changing the replication of DNA and inhibiting the growth of the tumor cells, which is the basis of designing new and more efficient anticancer drugs, where their effectiveness depends on the mode and affinity of the binding [28,29]. Therefore, the binding studies of metal complexes to DNA are considered to be highly important in the development of new anticancer drugs.

Electronic absorption spectroscopy is an effective method to examine the binding modes of metal complexes with DNA. Compounds binding through intercalation usually results in hypochromism with or without small red or blue shift, since the intercalative mode involves a strong interaction between the planar aromatic chromophore and the base pairs of DNA [30]. The results of absorption spectra of the compounds in the absence and presence of CT-DNA are given in Fig. 6. Upon increasing the concentration of DNA to the test compounds, the absorption bands of the ligands **1** and **2** exhibited hypochromism of 5.65 % and 17.34 % with blue shifts of 2 nm at 310 and 280 nm, whereas the absorption bands of complexes **3** and **4** exhibited a hypochromism of about 17.34 % at 366 nm and 24.92 % at 363 nm with blue shifts of 3 nm, respectively. However, complexes **5** at 356 nm and **6** at 366 nm exhibited a hypochromism of about 8.55 % and 3.71 % with red shifts of 4 and 2 nm, respectively. These results suggested an intimate association of the test compounds with CT-DNA, and it is also likely that these compounds bind to the DNA helix via intercalation. After the compounds intercalate to the base pairs of DNA, the π^* orbital of the intercalated compounds could couple with π orbitals of the base pairs, thus decreasing the $\pi \rightarrow \pi^*$ transition energies, hence resulting in hypochromism [31]. In order to compare quantitatively the binding strength of the compounds, the intrinsic binding constants (K_b) of them with CT-DNA were determined from the following equation.

$$[DNA]/(\varepsilon_a - \varepsilon_f) = [DNA]/(\varepsilon_b - \varepsilon_f) + 1/K_b\,(\varepsilon_b - \varepsilon_f)$$

where [DNA] is the concentration of DNA in base pairs and the apparent absorption coefficient ε_a, ε_f and ε_b correspond to A_{obs}/[compound], the extinction coefficient of the free compound and the extinction coefficient of the compound when fully bound to DNA, respectively. The plot of $[DNA]/(\varepsilon_a - \varepsilon_f)$ versus [DNA] gave a slope and the intercept

which are equal to $1/(\varepsilon_b - \varepsilon_f)$ and $1/K_b\ (\varepsilon_b - \varepsilon_f)$, respectively; K_b is the ratio of the slope to the intercept. The magnitudes of intrinsic binding constants (K_b) were calculated to be 1.7(±0.08) X 10^4 M^{-1}, 4.6(±0.12) X 10^3 M^{-1}, 3.4(±0.17) X 10^5 M^{-1}, 3.0(±0.09) X 10^5 M^{-1}, 6.3(±0.10) X 10^4 M^{-1} and 2.6(±0.16) X 10^4 M^{-1} for compounds **1**, **2**, **3**, **4**, **5** and **6** respectively. The observed values of K_b revealed that the ruthenium(II) complexes (**3** - **6**) bind strongly than the respective ligands (**1** and **2**) to DNA via intercalative mode. From the results obtained, it has been found that complex **3** strongly bound with CT-DNA relative to that with **4**, **5** and **6**, and the order of binding affinity is **3 > 4 > 5 > 6 > 1 > 2**.

3.5.2. DNA cleavage study by gel electrophoresis

Suitably designed metal complexes, after binding to DNA, can induce several changes in the DNA conformation, such as bending, 'local denaturation' (overwinding and underwinding), intercalation, micro loop formation and subsequent DNA shorting lead to decrease in molecular weight of DNA [32]. The ability of metal complexes to perform DNA cleavage is generally monitored by agarose gel electrophoresis and in the present work CT DNA was chosen to investigate its cleavage. The cleavage experiments were carried out in the absence and presence of activating agent, H_2O_2 under aerobic conditions and are shown in Fig 7 and 8 respectively. Fig. 7, shows the hydrolytic cleavage activity of the complexes, **3**-**6** at 40 µM. A control experiment using DNA alone does not show any significant cleavage of DNA (Lane 1). Further, when DNA is allowed to interact with the complexes, no considerable difference in the intensity of the bands for metal bound DNA as compared to control DNA was observed. This result suggests that the nuclease activity of the complexes does not involve by hydrolytic pathway. These experimental facts demonstrated that a combination of both the ruthenium complexes and activating agent, H_2O_2 are required to show effective cleavage of CT DNA. Fig. 8 reveals that the oxidative cleavage of CT DNA induced by complexes, **3**-**6** in the presence of H_2O_2. Control experiment using DNA alone (Lane 1 & 9) and DNA with H_2O_2 (Lane 2 and 10) does not show any significant cleavage of CT-DNA even on longer exposure time. When the DNA is allowed to interact with the complexes (**3**-**6**) at various concentrations (30, 60 and 90 µM), a substantial decrease in the intensities of the bands for the metal bound DNA as compared to untreated control DNA was observed, which suggests the cleavage of DNA by metal complexes [33]. As can be seen from Lanes 5, 8, 13 and 16 of complexes **3**, **4**, **5** and **6** respectively, the bands were completely disappeared, indicating the sufficient cleavage of DNA by ruthenium(II)

complexes at 90 μM concentration. Interestingly, the complex, **3** shows potential nuclease activity against DNA at low concentration, 30 μM itself, indicates a superior DNA cleavage than the other complexes. The cleavage activity may be due to the intercalative interaction of the complexes with the DNA strands in the presence of H_2O_2 induces oxidative DNA cleavage [33].

3.5.2. Antioxidant activity

Since the DNA interaction experiments conducted so far revealed that the compounds exhibit good DNA binding affinity and good cleavage activity, it is considered worthwhile to study the antioxidant activity of these compounds. 2,2-Diphenyl-2-picryl-hydrazyl (DPPH) assay is widely used for assessing the ability of radical scavenging activity and it is measured in terms of IC_{50} values. Because of the presence of odd electron, DPPH shows a strong absorption band at 517 nm in the visible spectrum. As this electron becomes paired off in the presence of a free radical scavenger, this absorption vanishes, and the resulting decolourization is stoichiometric with respect to the number of electrons taken up. The DPPH assay of the tested compounds is shown in Fig. 9, it is seen from the results that the all the complexes exhibited moderate activity compared to the standard Ascorbic acid (Aca). The IC_{50} values indicated that the compounds showed antioxidant activity in the order of **3** > **4** > **5** > **6** > **1** > **2**. Complex **3** showed a higher antioxidant activity compared to other three complexes. From the above results, the scavenging effect of the free ligands is significantly less when compared to that of their corresponding ruthenium(II) complexes which is due to the chelation of the organic ligands with the ruthenium(II) ion.

3.5.3. In vitro anticancer activity evaluation

Cancer is a complex disease that is normally associated with a wide range of escalating effects both at the molecular and cellular levels. Synthesized metal complexes have been successfully used as anticancer drugs with high selectivity against malignant cells and with the ability to repress tumor metastasis. As candidates for such drugs, cytotoxic, antitumor or anticancer natural products have been often sought and the synthesized complexes have been used as therapeutics. The ligands and complexes were evaluated for their cytotoxicity against human breast cancer cell line (MCF-7) by means of MTT assay method that measures mitochondrial dehydrogenase activity as an indication of cell viability. The results were analyzed by means of cell viability curves and expressed with IC_{50} values in

the studied concentration range from 0.1–100 μM. The activity that corresponds to the inhibition of cancer cell growth at a maximum level is shown in Fig. 10, Table 5. Upon increasing the concentration of complexes, the results of MTT assays revealed that the complex **3** showed a higher cytotoxic effect followed by **4**. Complexes, **5** and **6** showed significant IC_{50} values but the cytotoxic effect of these complexes are less when compared to the other two complexes **3** and **4**. It is to be noted that the ligands does not show any significant activity (IC_{50} 100 μM), which confirmed that the chelation of the ligands with the ruthenium(II) ion is the only responsible factor for the observed cytotoxic property of the complexes. Comparison of the anticancer activity of the ruthenium(II) complexes reveal that upon changing the thiosemicarbazone moieties and ancillary ligands the activity of the complexes gets varied. The complexes of chlorobenzaldehyde thiosemicarbazone moiety exhibited higher cytotoxic effects than the complexes of nitrobenzaldehyde thiosemicarbazone. Moreover, the complexes containing triphenylphosphine as a co-ligand showed better cytotoxic effects than the complexes containing triphenylarsine. For clinical purposes, the compounds that show cytotoxicity in shorter time periods are preferred. The data obtained for our compounds showed cytotoxicity with short incubation period (48 h) and hence the data are highly significant. The findings of the *in vitro* cytotoxic activities confirm the binding of the complexes to DNA, which consequently leads to cell death.

4. Conclusion

Four ruthenium(II) complexes bearing NS-thiosemicarbazone ligands and the PPh_3/ $AsPh_3$ co-ligands are synthesized and characterized by various spectroscopic techniques. Thiosemicarbazone ligands have also been characterized by crystallographically. The complexes are tentatively assigned an octahedral geometry. All the newly synthesized compounds have been subjected to examine their biological property like DNA binding, DNA cleavage, antioxidant and cytotoxicity under *in vitro* experimental conditions. The DNA binding ability of the ligands and complexes has been assessed by absorption spectra which inferred an intercalative mode of binding with binding constants ranging from 10^3-10^5 M^{-1}. The DNA cleavage capabilities of complexes in the presence of H_2O_2 revealed their potential nuclease activity to cleave CT DNA. The complex **3** showed superior cleavage activity at low concentration than the other complexes. The antioxidant activity showed that all the ruthenium(II) complexes can serve as potential antioxidants than the ligands against DPPH radical in the order **3** > **4** > **5** > **6** > **1** > **2**. In addition, the *in vitro* cytotoxicity of the

complexes possesses significant activity against MCF-7 cell line. Complex **3** exhibited good cytotoxic effect than the other complexes and ligands. At this juncture, it is notable to mention that the major chemical and biological findings of this study throw some light on the potential of these complexes in a reasonable range of concentrations under *in vitro* conditions. In our opinion, the significant outcome of the present investigation regarding the abilities of ruthenium organometallic thiosemicarbazone complexes towards various biological evaluations is that the substitution of chlorobenzaldehyde in the thiosemicarbazone moiety with triphenylphosphine as co ligand led to an increased interaction with DNA, free radical and tumor cell line than the rest of the complexes.

Acknowledgements

Financial assistance received from the Council of Scientific and Industrial Research, New Delhi, India [Grant No. 01(2308)/09/EMR-II] is gratefully acknowledged.

Appendix A. Supplementary data

CCDC 893840 and 893999 contains the crystallographic data for compounds **1** and **2** respectively. These data can be obtained free of charge via http://www.ccdc.cam.ac.uk/conts/retrieving.html, or from the Cambridge Crystallographic Data Centre, 12 Union Road, Cambridge CB2 1EZ, UK; fax: (+44) 1223-336-033; or e-mail: deposit@ccdc.cam.ac.uk.

References

[1] M.J. Hannon, Pure Appl. Chem. 79 (2007) 2243-2261.

[2] T. Stringer, B. Therrien, D.T. Hendricks, H. Guzgay, G.S. Smith, Inorg. Chem. Comm. 14 (2011) 956-960.

[3] C. Metcalfe, J.A. Thomas, Chem. Soc. Rev. 32 (2003) 215-224.

[4] S.A. Ezadyar, A.S. Kumbhar, A.A. Kumbhar, A. Khan, Polyhedron 36 (2012) 45-55.

[5] A.I. Matesanz, C. Hernandez, A. Rodriguez, P. Souza, J. Inorg. Biochem. 105 (2011) 1613-1622.

[6] H. Beraldo, D. Gambino, Mini Rev. Med. Chem. 4 (2004) 31-39.

[7] D.K. Dermertzi, M.A. Demertzis, J.R. Miller, C.S. Frampton, J.P. Jasinski, D.X. West, J. Inorg. Biochem. 92 (2002) 137-140.

[8] J.G. Tojal, A.G. Orad, J.L. Serra, J.L. Pizarro, L. Lezamma, M.I. Arriortua, T. Rojo, J. Inorg. Biochem. 75 (1999) 45-54.

[9] R.N. Prabhu, D. Pandiarajan, R. Ramesh, J. Organomet. Chem. 694 (2009) 4170-4177.

[10] J.S. Casas, M.S. Garcia-Tasende, J. Sordo, Coord. Chem. Rev. 209 (2000) 197-261.

[11] A.I. Vogel, Textbook of Practical Organic Chemistry, fifth ed., Longman, London, 1989.

[12] K. Natarajan, U. Agarwala, Inorg. Nucl. Chem. Letters 14 (1978) 7-10.

[13] R.A. Sanchez-Delgado, W.Y. Lee, S.R. Choi, Y. Cho, M.J. Jun, Trans. Met. Chem. 16 (1991) 241-244.

[14] Siemens, SMART and SAINT, Area detector control and Integration software, Siemens Analytical X-ray Instruments Inc., Madison, WI, USA, 1996.

[15] G.M. Sheldrick, SADABS, Program for empirical absorption correction of area detector data, University of Gottingen, Germany, 1997.

[16] G.M. Sheldrick, SHELXS-97, Program for the solution of crystal structures, University of Gottingen, Gottingen, Germany, 1997.

[17] G.M. Sheldrick, SHELXL-97, A Program for the solution of crystal structures, University of Gottingen, Gotingen, Germany, 1997.

[18] K. Elizabeth, M.N.A. Rao, Int. J. Pharmaceut. 58 (1990) 237-240.

[18] M.S. Blois, Nature 181 (1958) 1199-1200.

[19] T. Mossman, J. Immnol. Methods 65 (1983) 55-63.

[20] S. Singh, F. Athar, M.R. Maurya, A. Azam, Eur. J. Med. Chem. 41 (2006) 592-598.

[21] V. Mahalingam, N. Chitrapriya, F.R. Fronczek, K. Natarajan, Polyhedron 29 (2010) 3363-3371.

[22] A. Manimaran, C. Jayabalakrishnan, J. Adv. Res. 3 (2012) 233-243.

[23] R.V. Sing, S.C. Joshi, A. Garaj, P. Naqpal, Appl. Organomet. Chem. 16 (2002) 713-720.

[24] G. Raja, N. Sathya, C. Jayabalakrishnan, J. Coord. Chem. 64 (2011) 817-831.

[25] M. Maji, S. Ghosh, S.K. Chattopaghyay, T.C.W. Mak, Inorg. Chem. 36 (1997) 2938-2943.

[26] N. Chitrapriya, T.S. Kamatchi, M. Zeller, H. Lee, K. Natarajan, Spectrochim. Acta A 81 (2011) 128-134.

[27] P. Viswanathamurthi, M. Muthukumar, J. Chem. Sci. 123 (2011) 567-576.

[28] A.M. Pyle, T. Morri, J.K. Barton, J. Am. Chem. Soc. 112 (1990) 9432-9434.

[29] J.K. Barton, J.M. Goldberg, C.V. Kumar, N.J. Turro, J. Am. Chem. Soc. 108 (1986) 2081-2088.

[30] Z.-C. Liu, B.-D. Wang, B. Li, Q. Wang, Z.-Y. Yang, T.-R. Li, Y. Li, Eur. J. Med. Chem. 45 (2010) 5353-5361.

[31] D.S. Raja, N.S.P. Bhuvanesh, K. Natarajan, Eur. J. Med. Chem. 46 (2011) 4584-4594.

[32] N.V. Kulkarni, A. Kamath, S. Budagumpi, V.K. Revankar, J. Mol. Str. 1006 (2011) 580-588.

[33] A.H. Pathan, R.P. Bakale, G.N. Naik, C.S. Frampton, K.B. Gudasi, Polyhedron 34 (2012) 149-156.

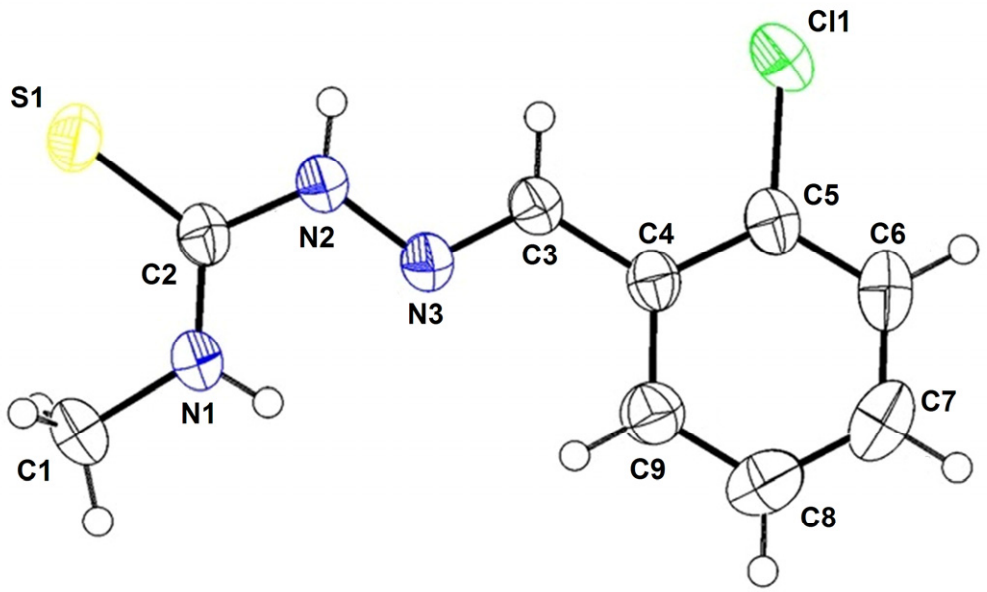

Fig. 1. ORTEP diagram of **1** with thermal ellipsoid at 50% probability

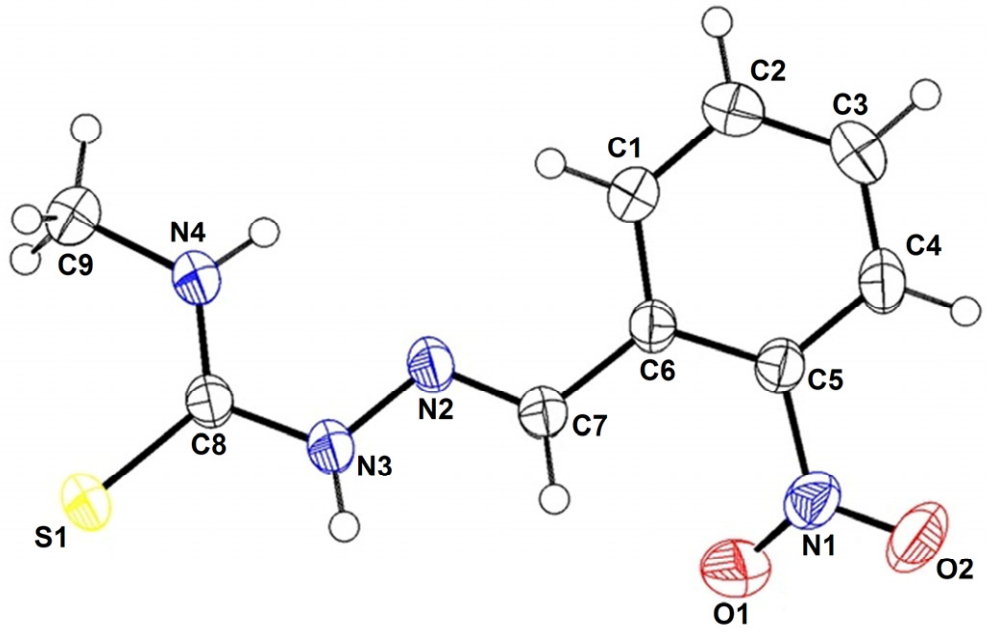

Fig. 2. ORTEP diagram of **2** with thermal ellipsoid at 50% probability.

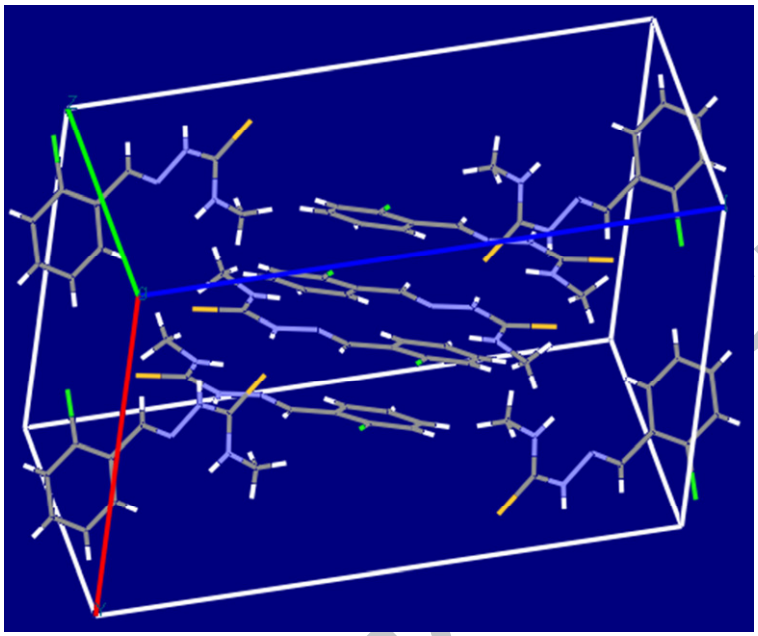

Fig. 3. Crystal packing diagram of **1**

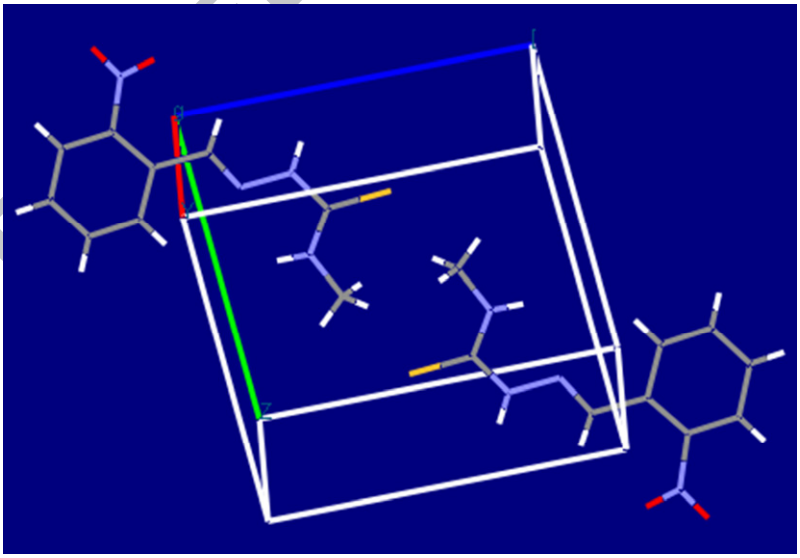

Fig. 4. Crystal packing diagram of **2**

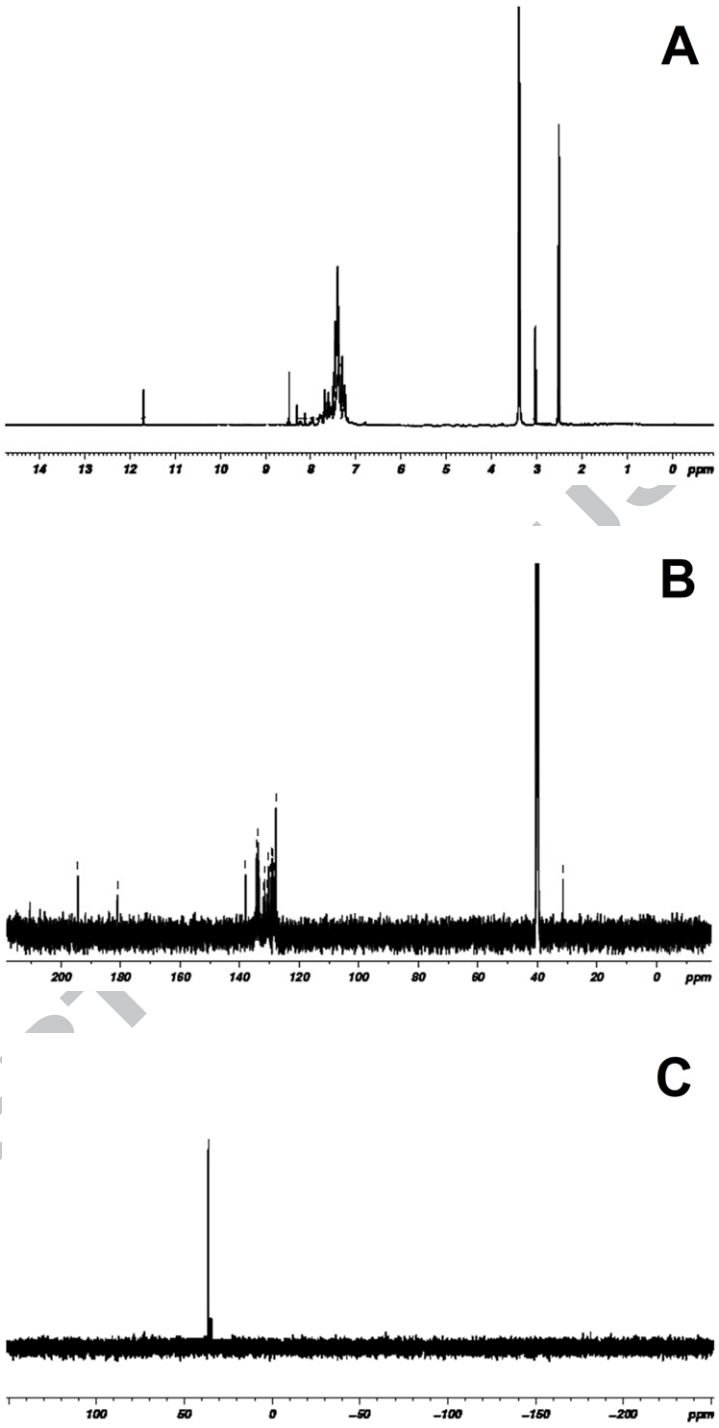

Fig. 5. ^{1}H (A), ^{13}C (B) and ^{31}P (C) NMR spectrum of the complex **3**

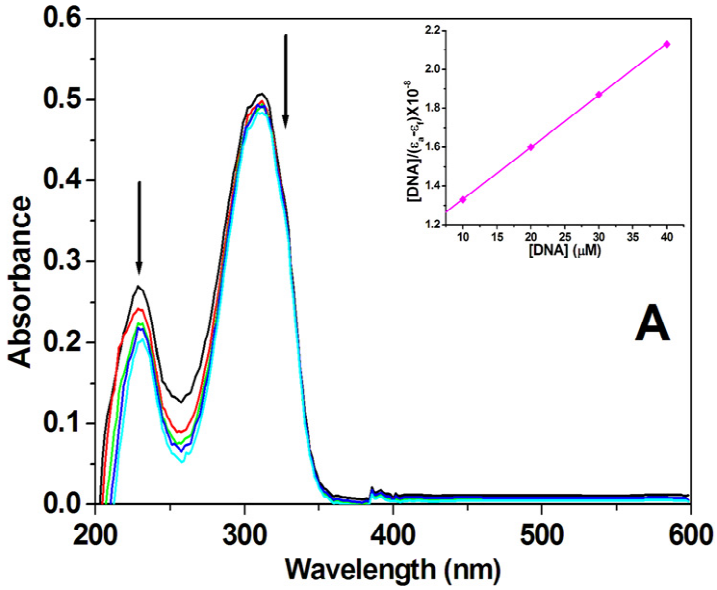

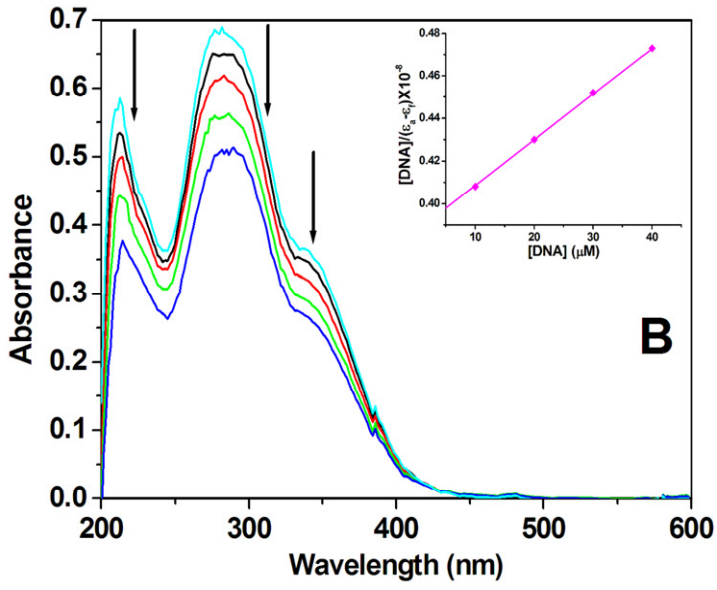

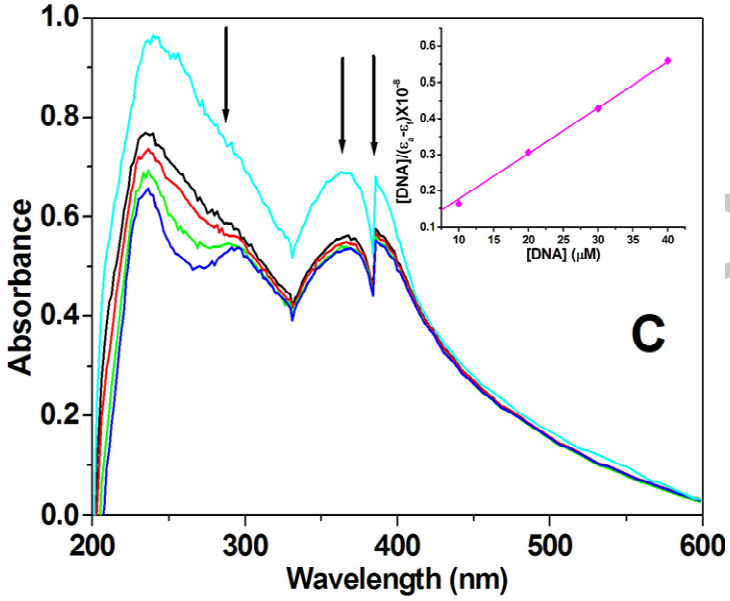

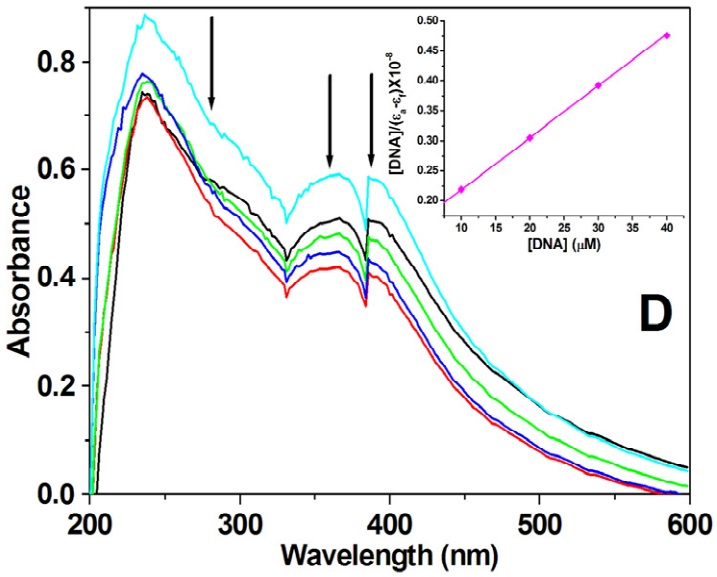

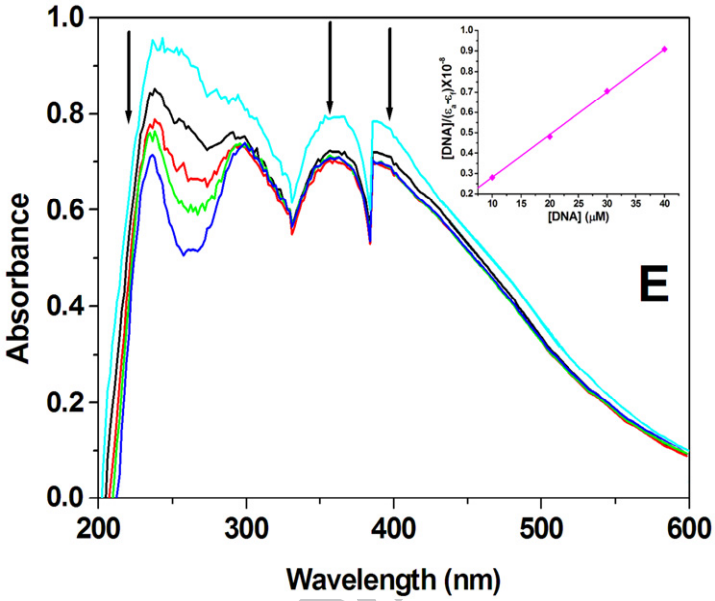
Absorbance
Wavelength (nm)
[DNA]/(ε_a-ε_f)X10^-8
[DNA] (μM)
E

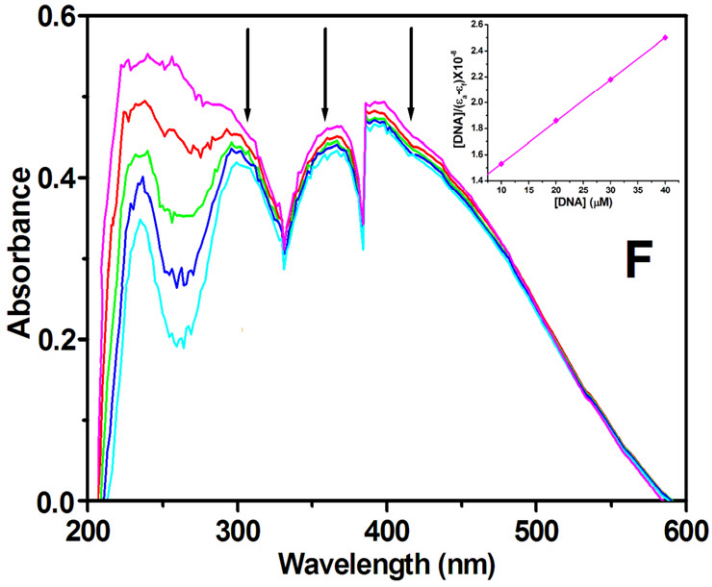
Absorbance
Wavelength (nm)
[DNA]/(ε_a-ε_f)X10^-8
[DNA] (μM)
F

Fig. 6. Electronic spectra of compounds **1** (A), **2** (B), **3** (C), **4** (D), **5** (E) and **6** (F) in Tris-HCl buffer upon addition of CT-DNA. [Complex] = 25 µM, [DNA] = 0-40 µM. Arrow shows the absorption intensities decrease upon increasing DNA concentrations
(Inset: Plot between [DNA] and [DNA]/ $[\varepsilon_a-\varepsilon_f]$ X 10^{-8}).

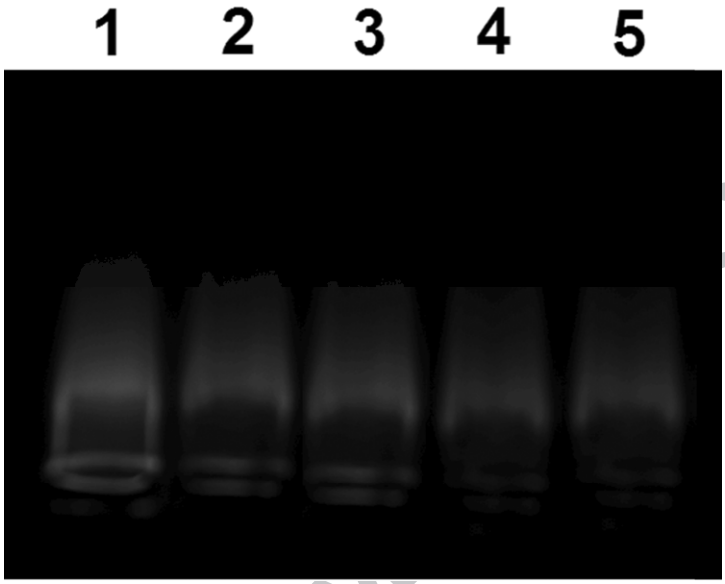

Fig. 7. Gel electrophoresis diagram showing the hydrolytic cleavage of CT-DNA (30 µM) incubated at 37 °C for a period of 2 h at a concentration of 40 µM of complex **3**-**6** in 5% DMSO and 95% 5 mM Tris-HCl/50 mM NaCl buffer at pH 7.2. Lane 1: Control,
Lanes 2-5: DNA + complexes **3**-**6**, respectively.

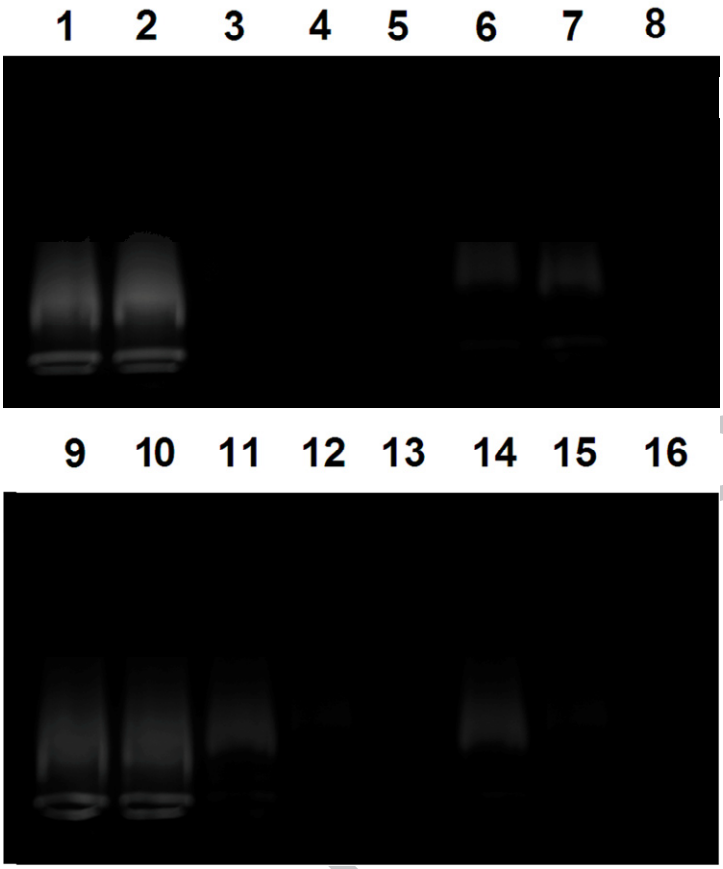

Fig. 8. Gel electrophoresis diagram showing the oxidative cleavage of CT-DNA (30 µM) by complexes **3**-**6** in 5% DMSO and 95% 5 mM Tris-HCl/50 mM NaCl buffer at pH 7.2 in the presence of H_2O_2 (60 µM) as a co-oxidant incubated at 37 °C for a period of 2 h. Lane 1 and 9: DNA. Lanes 2 and 10: DNA + H_2O_2. Lane 3-5: **3** (30, 60 and 90 µM) + DNA + H_2O_2. Lane 6-8: **4** (30, 60 and 90 µM) + DNA + H_2O_2. Lane 11-13: **5** (30, 60 and 90 µM) + DNA + H_2O_2. Lane 14-16: **6** (30, 60 and 90 µM) + DNA + H_2O_2.

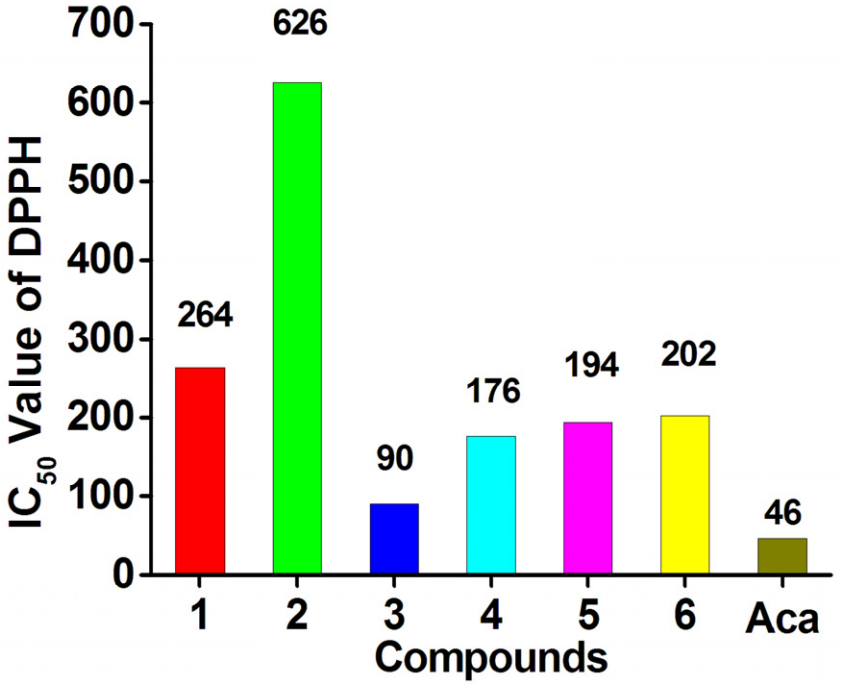

Fig. 9. Antioxidant activity of compounds

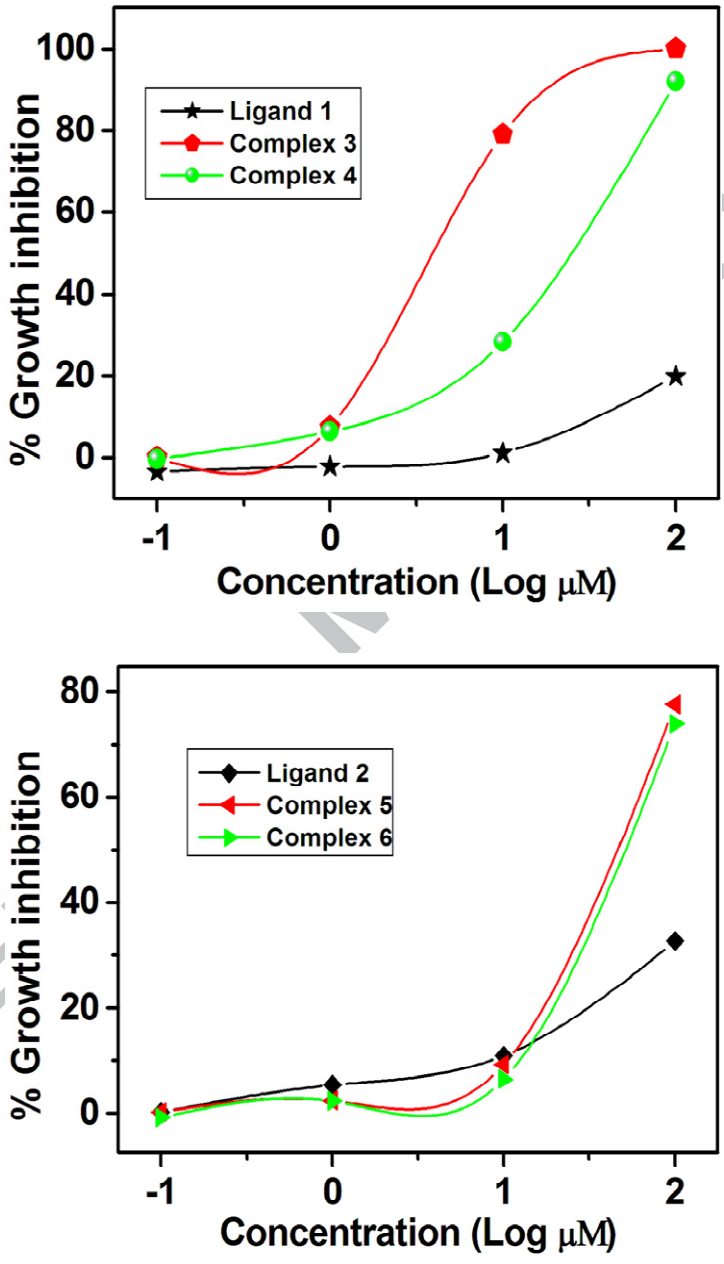

Fig. 10. % Growth inhibition of MCF-7 cell line as a function of concentration of the compounds **1**-**6**

Table 1 Experimental Data for Crystallographic Analyses.

Compound	**1**	**2**
CCDC Number	893840	893999
Empirical formula	$C_9H_{10}ClN_3S$	$C_9H_{10}N_4O_2S$
Formula weight	227.71	238.27
Temperature (K)	296(2)	296(2)
Wavelength (Å)	0.71073	0.71073
Crystal system	Monoclinic	Triclinic
Space group	C2/c	P-1
Unit cell dimensions		
a (Å)	14.3409(11)	7.3403(4)
b (Å)	8.0487(7)	8.0726(4)
c (Å)	18.6839(14)	10.1536(5)
α (°)	90	87.194(2)
β (°)	90.868(2)	70.544(2)
γ (°)	90	72.861(2)
Volume ($Å^3$)	2156.4(3)	541.30(5)
Z	8	2
Density (cal.) (mg/m^3)	1.403	1.462
Abs. coefficient (mm^{-1})	0.511	0.290
F(000)	944	248
Crystal size (mm^3)	0.40 x 0.35 x 0.30	0.40 x 0.30 x 0.20
θ range for data collection (°)	2.18 to 28.29	2.64 to 28.16
Index ranges	-18<=h<=17, -10<=k<=10, -24<=l<=24	-9<=h<=9, -10<=k<=10, -13<=l<=13
Reflections collected	9667	8930
Independent reflections	2652 [R(int) = 0.0315]	2585 [R(int) = 0.0196]
Absorption correction	Semi-empirical from equivalents	Semi-empirical from equivalents
Max. and min. transmission	0.8617 and 0.8216	0.9443 and 0.8928
Refinement method	Full-matrix least-squares on F^2	Full-matrix least-squares on F^2
Data/restraints/parameters	2652 / 0 / 129	2585 / 0 / 146
Goodness-of-fit on F^2	1.130	1.028
Final R indices [I>2σ(I)]	R1 = 0.0333, wR2 = 0.1010	R1 = 0.0337, wR2 = 0.0947
R indices (all data)	R1 = 0.0400, wR2 = 0.1164	R1 = 0.0377, wR2 = 0.0992

Table 2 Selected bond lengths [Å]

1		**2**	
Cl(1)-C(5)	1.7357(17)	C(1)-C(2)	1.3783(18)
S(1)-C(2)	1.6884(14)	C(1)-C(6)	1.3960(17)
N(1)-C(2)	1.321(2)	C(1)-H(1)	0.9300
N(1)-C(1)	1.4474(19)	C(2)-C(3)	1.384(2)
N(1)-H(1)	0.8600	C(2)-H(2)	0.9300
N(2)-C(2)	1.3540(17)	C(3)-C(4)	1.377(2)
N(2)-N(3)	1.3696(17)	C(3)-H(3)	0.9300
N(2)-H(2)	0.8600	C(4)-C(5)	1.3893(17)
N(3)-C(3)	1.2764(18)	C(4)-H(4)	0.9300
C(1)-H(1A)	0.9600	C(5)-C(6)	1.3999(15)
C(1)-H(1B)	0.9600	C(5)-N(1)	1.4656(16)
C(1)-H(1C)	0.9600	C(6)-C(7)	1.4700(15)
C(3)-C(4)	1.4616(19)	C(7)-N(2)	1.2761(15)
C(3)-H(3)	0.9300	C(7)-H(7)	0.9300
C(4)-C(5)	1.3951(19)	C(8)-N(4)	1.3224(16)
C(4)-C(9)	1.396(2)	C(8)-N(3)	1.3572(15)
C(5)-C(6)	1.381(2)	C(8)-S(1)	1.6834(11)
C(6)-C(7)	1.373(3)	C(9)-N(4)	1.4522(16)
C(6)-H(6)	0.9300	C(9)-H(9A)	0.9600
C(7)-C(8)	1.382(3)	C(9)-H(9B)	0.9600
C(7)-H(7)	0.9300	C(9)-H(9C)	0.9600
C(8)-C(9)	1.380(2)	N(1)-O(1)	1.2232(16)
C(8)-H(8)	0.9300	N(1)-O(2)	1.2256(15)
C(9)-H(9)	0.9300	N(2)-N(3)	1.3664(13)
		N(3)-H(3N3)	0.8600
		N(4)-H(4N4)	0.8600

Table 3 Selected bond angles [°]

1		**2**	
C(2)-N(1)-C(1)	124.55(14)	C(2)-C(1)-C(6)	121.93(11)
C(2)-N(1)-H(1)	117.7	C(2)-C(1)-H(1)	119.0
C(1)-N(1)-H(1)	117.7	C(6)-C(1)-H(1)	119.0
C(2)-N(2)-N(3)	119.25(12)	C(1)-C(2)-C(3)	120.31(12)
C(2)-N(2)-H(2)	120.4	C(1)-C(2)-H(2)	119.8
N(3)-N(2)-H(2)	120.4	C(3)-C(2)-H(2)	119.8
C(3)-N(3)-N(2)	115.70(12)	C(4)-C(3)-C(2)	119.88(12)
N(1)-C(1)-H(1A)	109.5	C(4)-C(3)-H(3)	120.1
N(1)-C(1)-H(1B)	109.5	C(2)-C(3)-H(3)	120.1
H(1A)-C(1)-H(1B)	109.5	C(3)-C(4)-C(5)	119.00(12)
N(1)-C(1)-H(1C)	109.5	C(3)-C(4)-H(4)	120.5
H(1A)-C(1)-H(1C)	109.5	C(5)-C(4)-H(4)	120.5
H(1B)-C(1)-H(1C)	109.5	C(4)-C(5)-C(6)	122.81(11)
N(1)-C(2)-N(2)	116.62(13)	C(4)-C(5)-N(1)	115.88(10)
N(1)-C(2)-S(1)	124.28(11)	C(6)-C(5)-N(1)	121.27(10)
N(2)-C(2)-S(1)	119.11(11)	C(1)-C(6)-C(5)	116.01(11)
N(3)-C(3)-C(4)	120.10(13)	C(1)-C(6)-C(7)	119.20(10)
N(3)-C(3)-H(3)	119.9	C(5)-C(6)-C(7)	124.64(11)
C(4)-C(3)-H(3)	119.9	N(2)-C(7)-C(6)	118.24(10)
C(5)-C(4)-C(9)	117.43(13)	N(2)-C(7)-H(7)	120.9
C(5)-C(4)-C(3)	121.13(13)	C(6)-C(7)-H(7)	120.9
C(9)-C(4)-C(3)	121.44(13)	N(4)-C(8)-N(3)	116.84(10)
C(6)-C(5)-C(4)	121.83(15)	N(4)-C(8)-S(1)	123.79(9)
C(6)-C(5)-Cl(1)	117.85(12)	N(3)-C(8)-S(1)	119.36(9)
C(4)-C(5)-Cl(1)	120.32(12)	N(4)-C(9)-H(9A)	109.5
C(7)-C(6)-C(5)	119.39(16)	N(4)-C(9)-H(9B)	109.5
C(7)-C(6)-H(6)	120.3	H(9A)-C(9)-H(9B)	109.5
C(5)-C(6)-H(6)	120.3	N(4)-C(9)-H(9C)	109.5
C(6)-C(7)-C(8)	120.28(16)	H(9A)-C(9)-H(9C)	109.5
C(6)-C(7)-H(7)	119.9	H(9B)-C(9)-H(9C)	109.5
C(8)-C(7)-H(7)	119.9	O(1)-N(1)-O(2)	123.29(12)
C(9)-C(8)-C(7)	120.15(18)	O(1)-N(1)-C(5)	118.67(11)
C(9)-C(8)-H(8)	119.9	O(2)-N(1)-C(5)	117.98(12)
C(7)-C(8)-H(8)	119.9	C(7)-N(2)-N(3)	116.73(10)
C(8)-C(9)-C(4)	120.88(16)	C(8)-N(3)-N(2)	119.28(10)
C(8)-C(9)-H(9)	119.6	C(8)-N(3)-H(3N3)	120.4

C(4)-C(9)-H(9)	119.6	N(2)-N(3)-H(3N3)	120.4
		C(8)-N(4)-C(9)	123.48(11)
		C(8)-N(4)-H(4N4)	118.3
		C(9)-N(4)-H(4N4)	118.3

Table 4 Selected torsion angles [°]

1		**2**	
H(1)-N(1)-C(1)-H(1A)	125.8(2)	C(6)-C(1)-C(2)-C(3)	-2.0(2)
H(1)-N(1)-C(1)-H(1C)	-114.1(2)	C(1)-C(2)-C(3)-C(4)	1.5(2)
C(2)-N(1)-C(1)-H(1B)	-174.2(2)	C(2)-C(3)-C(4)-C(5)	0.7(2)
H(1)-N(1)-C(2)-S(1)	-177.5(1)	C(3)-C(4)-C(5)-C(6)	-2.5(2)
C(1)-N(1)-C(2)-N(2)	-177.4(2)	C(3)-C(4)-C(5)-N(1)	174.98(12)
C(2)-N(2)-N(3)-C(3)	175.6(1)	C(2)-C(1)-C(6)-C(5)	0.33(18)
H(2)-N(2)-C(2)-N(1)	179.5(1)	C(2)-C(1)-C(6)-C(7)	176.07(12)
N(3)-N(2)-C(2)-S(1)	179.6(1)	C(4)-C(5)-C(6)-C(1)	1.94(18)
N(2)-N(3)-C(3)-C(4)	179.0(1)	N(1)-C(5)-C(6)-C(1)	-175.39(11)
N(3)-C(3)-C(4)-C(5)	171.9(1)	C(4)-C(5)-C(6)-C(7)	-173.54(11)
N(3)-C(3)-C(4)-C(9)	-8.9(2)	N(1)-C(5)-C(6)-C(7)	9.13(18)
H(3)-C(3)-C(4)-C(5)	-8.1(2)	C(1)-C(6)-C(7)-N(2)	15.00(17)
H(3)-C(3)-C(4)-C(9)	171.1(1)	C(5)-C(6)-C(7)-N(2)	-169.65(11)
C(3)-C(4)-C(5)-C(l1)	-3.3(2)	C(4)-C(5)-N(1)-O(1)	-148.74(13)
C(3)-C(4)-C(5)-C(6)	177.1(1)	C(6)-C(5)-N(1)-O(1)	28.77(17)
C(9)-C(4)-C(5)-C(l1)	177.5(1)	C(4)-C(5)-N(1)-O(2)	28.70(16)
C(3)-C(4)-C(9)-C(8)	-176.9(2)	C(6)-C(5)-N(1)-O(2)	-153.79(12)
C(5)-C(4)-C(9)-H(9)	-177.8(1)	C(6)-C(7)-N(2)-N(3)	-176.86(10)
C(l1)-C(5)-C(6)-C(7)	-179.2(1)	N(4)-C(8)-N(3)-N(2)	1.15(17)
C(4)-C(5)-C(6)-H(6)	-179.7(2)	S(1)-C(8)-N(3)-N(2)	179.68(8)
C(5)-C(6)-C(7)-H(7)	-178.8(2)	C(7)-N(2)-N(3)-C(8)	178.73(11)
H(6)-C(6)-C(7)-C(8)	-178.8(2)	N(3)-C(8)-N(4)-C(9)	176.90(12)
C(6)-C(7)-C(8)-H(8)	179.0(2)	S(1)-C(8)-N(4)-C(9)	-1.55(19)
H(7)-C(7)-C(8)-C(9)	179.0(2)		
C(7)-C(8)-C(9)-H(9)	179.2(2)		
H(8)-C(8)-C(9)-C(4)	179.2(2)		

Table 5 Cytotoxic activity of the ligands and ruthenium(II) complexes against the cancer cell line, MCF-7.

Compounds	IC_{50} (μM)
1	>100
2	>100
3	4.5
4	18.99
5	44.19
6	52.12

Graphical Abstract

Four new ruthenium(II) complexes with benzaldehyde 4-methyl-3-thiosemicarbazones were prepared and fully characterized by various spectro-analytical techniques. The molecular structure of HL^1 and HL^2 were determined by single crystal X-ray diffraction method. The ligands act as bidentate, monobasic chelating ligands with S and N as the donor sites in all the complexes studied. DNA binding of the ligands and complexes were investigated by absorption spectroscopy which indicated that the complexes bind to DNA *via* intercalation. The oxidative cleavage of the complexes with CT-DNA inferred that the effects of cleavage are dose dependent. Further, *in vitro* antioxidant and anticancer studies were carried out for the ligands and ruthenium(II) complexes.

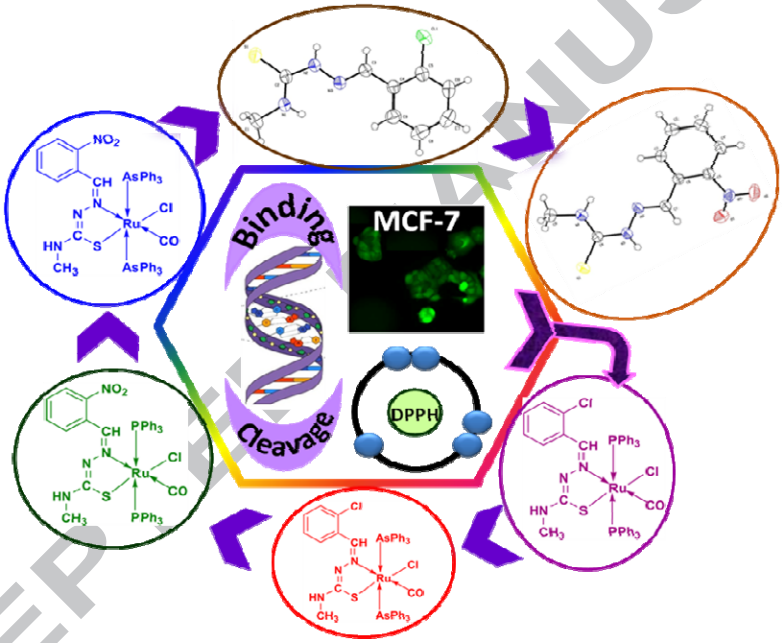

Highlights

- Molecular structure of Ligands was elucidated by X- ray diffraction study.
- The ligands and complexes interact with CT-DNA, intercalatively.
- The complexes can efficiently cleave CT-DNA via oxidative cleavage.
- The complexes possess significant antioxidative property against DPPH radical.
- The complex **3** shows higher IC_{50} value than the other complexes against tumor cells.